



A Statistics-Based Correlation for the Assessment of Water-Based Mud Performance: Yield Point Prediction

Fahd Saeed Alakbari¹ · Mysara Eissa Mohyaldinn^{1,2} · Syed Mohammad Mahmood^{1,2} · Anas Mohammed Hassan³ · Rahman Ashena⁴ · Amin Al-Fakih^{5,6}

Received: 24 July 2023 / Accepted: 22 July 2024
© King Fahd University of Petroleum & Minerals 2024

Abstract

A suitable design of drilling fluids is essential to improve the drilling efficiency and decrease drilling time/cost. Yield point is one of the important rheological properties of drilling fluids used to delineate the performance of a drilling fluid. Although laboratory measurements of the YP are possible, they are time-consuming and costly. Therefore, predicting YP at different conditions and additive concentrations is quite advantageous. This work used response surface methodology (RSM) to build an accurate correlation that predicts YP based on pressure, temperature, and concentrations of nanosilica, nanoclay, and bentonite. The correlation was statistically analyzed by validating it through the F-statistics test, ANOVA, fit statistics, Pareto chart, and diagnostics plots to increase its accuracy and degree of confidence. The YP correlation was verified by using unseen data to check its efficiency. The influences between the predictor and target variables were shown in the contour and 3D surface response plots. The correlation results fairly agree with the measured data with a Pearson's correlation coefficient of 0.9947. The results show that the temperature and concentrations of bentonite and nanosilica highly affect the YP in water-based drilling fluids.

Keywords Yield point (YP) · Rheological properties · Water based · Drilling fluid · Response surface methodology

Abbreviations

YP	Yield point
RSM	Response surface methodology
ANOVA	Analysis of variance

F-statistics	Fisher statistics
ECD	Equivalent circulation density
WBDFs	Water-based drilling fluids
COV	Coefficient of variance
ANN	Artificial neural network
MSE	Mean squared error
WBM	Water-based mud
R_{300} and R_{600}	Viscometer readings at 300 and 600 RPM (revolution per minute)
ANFIS	Adaptive neuro-fuzzy inference system
AAPE	Average absolute percentage error
RMSE	Root mean square error
COA	Cuckoo optimization algorithm
RF	Random forest
DT	Decision tree
MD	Mud density
MFV	Marsh funnel viscosity
pcf	Pounds per cubic foot
MPa	Megapascal
MW	Mud weight
MF	Marsh funnel
S%	Solid content

✉ Fahd Saeed Alakbari
fahd.akbari@utp.edu.my; alakbarifahd@gmail.com

- ¹ Centre of Flow Assurance, Institute of Subsurface Resources, Universiti Teknologi PETRONAS, 32610 Bandar Seri Iskandar, Perak Darul Ridzuan, Malaysia
- ² Petroleum Engineering Department, Universiti Teknologi PETRONAS, 32610 Bandar Seri Iskandar, Perak Darul Ridzuan, Malaysia
- ³ Petroleum Engineering Department, Khalifa University of Science and Technology, Abu Dhabi, United Arab Emirates
- ⁴ SEDA-Group, Houston, USA
- ⁵ Department of Civil and Environmental Engineering, King Fahd University of Petroleum and Minerals, 31261 Dhahran, Saudi Arabia
- ⁶ Interdisciplinary Research Center for Construction and Building Materials, King Fahd University of Petroleum and Minerals, 31261 Dhahran, Saudi Arabia



UHPC	Ultra-high-performance concrete
P	Pressure
T	Temperature
C_{ns}	Concentrations of nanosilica
C_{nc}	Concentrations of nanoclay
C_b	Concentrations of bentonite
p -value	Probability value
F -value	Fisher value
df	Degrees of freedom
3D	Three dimensions or three-dimensional
wt.%	Weight percent

1 Introduction

An appropriate drilling fluid design is essential to improve the drilling efficiency and decrease drilling time and cost [1]. Rheological properties of drilling fluids, such as yield point (YP), plastic viscosity, and apparent viscosity, are substantial parameters used to describe the rheological behavior of drilling fluids.

The YP measurements in the laboratory are time-consuming and costly. As a good alternative, predictive methods are often considered for predicting the YP of water-based drilling fluids (WBDFs) to achieve good drilling operation performance [2, 3].

Several published models claimed to predict drilling fluids' YP using an artificial neural network (ANN) approach. Razi et al. [4] model predicted the WBM's YP based on shear rate, temperature, and starch concentration with a mean squared error (MSE) of 0.009 and a correlation coefficient (R^2) of 0.986. Elkatatny et al. [5] model found the oil-based mud (OBM)'s YP based on the drilling fluid's Marsh funnel viscosity, density, and solid contents. They used 9000 data points to develop a mathematical model based on the weights and biases with an average absolute error of 3. Elkatatny and Mahmoud [6] model obtained the YP of the water-based drilling fluid based on the Marsh funnel viscosity, solid content, and mud density with an R^2 of 0.98. Abdelgawad et al. [7] also applied the ANN method to predict the YP of bentonite spud mud using the Marsh funnel viscosity, solid content, and mud density in the ranges (26–120) s, (0–24)%, (63–80) lb/ft³ as inputs. The model has an R^2 of 0.94 [7]. Gowida et al. [8] used the Marsh funnel viscosity and mud density in the ranges (26–135) s/quart and (64–155) lb/ft³ to predict the CaCl₂ brine YP, and the model has R^2 of 0.97.

Other published models also used an ANN approach to predict drilling fluids' YP. Gomaa et al. [9] model predicted the YP of the high overbalanced bridging mud using the Marsh funnel viscosity and mud density in the ranges (42–120) s/quart and (43–119) lb/ft³ as inputs of the model

with an R^2 of 0.97 and 0.96 for R_{300} and R_{600} [9]. Oguntade et al. [10] model predicted the mud with modified biopolymer's YP based on the water volume and the concentrations of bentonite and biopolymer with RMSEs of 0.96 and 0.8331 for 15 and 8 neurons and the R^2 s of 0.92 and 0.99 for 15 and 8 neurons. Gowida et al. [11] model found the high-bentonite mud's YP using the Marsh funnel viscosity and mud density in the ranges (45–150) s/quart and (64–73) lb/ft³ as inputs of the model with an R^2 of 0.92 [11]. Alsabaa and Elkatatny [12] model predicted the oil-based drilling fluid's YP as a function of the density of the drilling fluid and Marsh funnel in the ranges (76–120) pcf and (44–120) s with an average absolute percentage error (AAPE) of 4.85% and an R^2 of 0.91 [12]. Gouda et al. [13] used mud temperature, Marsh funnel viscosity, solid content percentage, and mud density in the ranges (60–170) °F, (40–85) sec/qrt, (14.5–36.6)%, and (10.2–13.85), respectively, as inputs to find the yield point for invert emulsion drilling fluid. The model has an AAPE of 3.18% and R^2 of 0.94 [13]. Mengich et al. [14] found the WBM's YP based on mud density, percent solids content, and Marsh funnel with a root mean square error (RMSE) of 10.149 and R^2 of 0.7013 [14]. Al-Obaidi et al. [15] model predicted the rheological properties of the water-based drilling fluid, namely YP using the mud weight (MW), Marsh funnel (MF), and solid content (S%) as inputs with an RMSE of 0.891 and an R^2 of 0.90 [15]. Ashadevi et al. [16] model found the rheological properties of the oil-based drilling fluid, such as YP. The temperature, mud density, and shear rate were used as inputs, and a dataset contains 40 data points. The model has RMSE and R^2 of 0.01 and 0.99, respectively [16].

Some existing studies used an adaptive neuro-fuzzy inference system (ANFIS) to predict drilling fluids' YP. Alsabaa et al. [17] used the Marsh funnel viscosity and mud density in the ranges (45–98) s/quart and (67–98) lb/ft³ as inputs to predict the YP of the inverted emulsion mud with an R^2 of 0.91 [17]. Abdelaal et al. [18] model predicted the viscometer readings at 300 and 600 RPM. After that, they predicted the rheological properties of synthetic oil-based drilling fluids, such as YP using the exciting correlation in the literature. The models were built based on the mud density (MD) and Marsh funnel viscosity (MFV) in the ranges (70–120) pcf and (27–120) sec/quart. The model has an R^2 of 0.96 and an average absolute percentage error of less than 7%.

Abdelaal et al. [19] also applied random forest (RF) and decision tree (DT) to predict the viscometer readings at 300 and 600 RPM. The models were also built based on the mud density (MD) and Marsh funnel viscosity (MFV) in the ranges (70–120) pcf and (27–120) sec/quart. The models have an R^2 of 0.954 and 0.955 for RF and DT, respectively, and an average absolute percentage error of 3.9% and 3.6% for RF and DT, respectively.



For predicting the drilling fluid (OBM)'s YP using the nonlinear regression models, Oliveira [20] used pressure and temperature as predictor variables. The model had R^2 s of 0.9009 and 0.9271 for the Newton and Levenberg–Marquardt nonlinear regression models. His research used data in the limited range of 200–450 °F and 5000–40000 psig. Fakoya and Ahmed [21] utilized the volume fraction of dispersed phase and temperature in the range (24–87) °C as inputs to determine the YP for the oil-based drilling fluid. Tchameni et al. [22] operated multiple nonlinear regression and ANN methods to obtain the YP for the waste vegetable oil biodiesel-modified water-based mud (WBM) based on biodiesel content and a aging temperature in the range (28–180) °C. The model has an MSE and R^2 of 8.9275 and 0.807 [22]. Ye et al. [23] used temperature and pressure in the ranges (60–160) °C and (0.1–150) MPa as inputs to predict the rheological properties of oil-based drilling fluids including the YP applying the regression. The model has an average error of 4.85% [23].

Davoodi et al. [24] used the cuckoo optimization algorithm (COA) to predict the rheological properties of water-based drilling fluids, like YP. The model was created based on the fluid density, solid percentage, and Marsh funnel viscosity in the ranges (70–148) pcf, (2.7–47.0)%, (36.0–78.0) sec/quart. The model has an RMSE of 0.6357 and R^2 of 0.8672 [24].

Okumo and Isehunwa [25] applied factorial design to obtain the YP for the WBM based on the concentration of starch and potash in the mud and its temperature. Their model had a coefficient of variance (COV) of 6.435%, the standard deviation per mean multiple by 100%.

Igwilo et al. [26] utilized the least square and Gaussian elimination methods to find the YP for the OBM based on mud temperature. The model had an R^2 of 0.8955, 0.9911, 0.9475, 0.9905, and 0.9846 for power, polynomial, exponential, linear, and logarithm regression types, respectively.

In the literature, previous studies used different methods to predict the drilling fluid's YP based on different inputs. However, this study used response surface methodology (RSM), which is unique since previous models are mostly based on ANN. Some models also used ANFIS, DT, and RF methods, but none used RSM. A new modeling approach can be a welcome addition to existing predictive tools. This technique is easier to use and more accurate than the previous ones. Previous studies used input parameters such as the concentration of starch in the mud and potash, temperature, Marsh funnel viscosity, solid content, mud density, water volume, and concentrations of bentonite and biopolymer in different ranges to predict the YP. In contrast, the proposed study used pressure (P), temperature (T), concentrations of nanosilica (C_{ns}), concentrations of nanoclay (C_{nc}), and concentrations of bentonite (C_b) in the ranges (14.70–500) psi, (85–250) F, (0–10) wt.%, (0–5) wt.%, (0–10) wt.%. Thus, the input

parameters used in the proposed model are more relevant as these parameters affect the drilling fluid's YP.

The relationship between parameters in various domains can be established using RSM models. RSM can model and optimize nonlinear relationships between variables, which is common in real-world systems. RSM facilitates the development of empirical models that can be used to predict the response for given levels of input variables. These models are often polynomial equations that are easier to interpret and use for prediction [27]. In the literature, the RSM was used successfully in many engineering applications. For example, the RSM was used by Moraveji and Naderi [28] to determine the optimal drilling penetration rate.

The main objective of this study is to develop a robust, accurate, and new correlation using RSM to predict the YP of WBMs. Five parameters are considered key features to predict the YP. Two features, i.e., pressure and temperature, are to represent the flow condition. The other three features, i.e., nanosilica, nanoclay, and bentonite concentrations, are present in the fluid composition. The developed correlation was evaluated using different approaches: analysis of variance, F-statistic test, fit statistics, Pareto chart, diagnostics plots, and perturbation plot. The YP correlation was also validated against the measured data to show high accuracy and more confidence. In addition, the RSM will be used to correlate the yield stress to the five parameters to show the influences between them.

2 Methodology

The block diagram of the methodology used to build the proposed response surface methodology (RSM) model, which predicts the YP of the water-based drilling fluid, is shown in Fig. 1. The block diagram involves the components: (1) data collection, (2) creating a YP model, (3) RSM model evaluation, (4) RSM model validation, (5) study effects of the predictors on YP, and comparison between the recent and proposed models. Firstly, the data were collected from the literature, and pressure (P), temperature (T), concentrations of nanosilica (C_{ns}), concentrations of nanoclay (C_{nc}), and concentrations of bentonite (C_b) as predictor variables and a YP as the target variable were used. After collecting the data, a model was created to predict the YP using the RSM method by applying the Design-Expert and Statistica software. The modeling of WBMs' rheological properties other than the yield point has been previously published [29]. Then, the created RSM model was evaluated using different techniques: analysis of variance (ANOVA), diagnostics plots, Pareto chart, and fit statistics. Next, the RSM model was validated by using some data not used to create the proposed RSM model. In the next stage, the YP model's contour and 3D plots of surface response were applied using Design-Expert

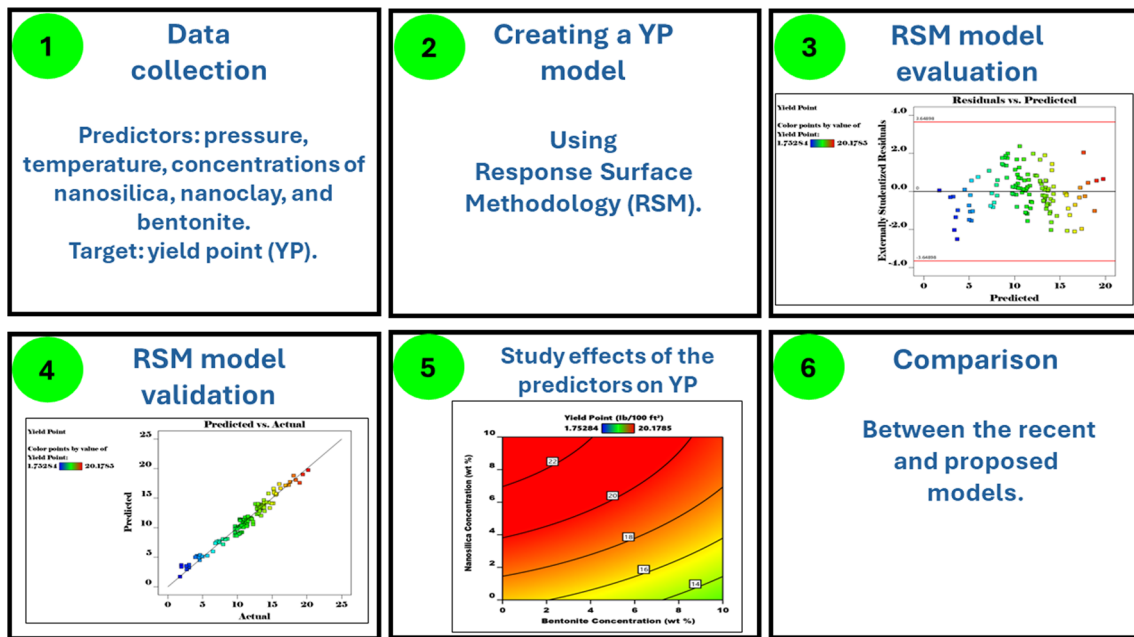


Fig. 1 Block diagram of the RSM model to predict the yield point

and Statistica software to evaluate the interactive relationships of predictors with the target. Finally, the RSM model and existing models in the literature to predict the YP of drilling fluid were compared.

2.1 Data Description

A total of 1256 data points were collected from the experimental measurements of the WBM to build the RSM model for predicting the YP [30]. The data comprise P , T , C_{ns} , C_{nc} , and C_b as predictor variables and a YP as the target variable. Table 1 displays the data ranges, as the collected data were split into two parts: 1176 data points for developing the model and 80 data points for verification.

2.2 Yield Point Correlation Development Using Response Surface Methodology (RSM)

A well-known method for performing the design of experiments (DOE) is the RSM, i.e., response surface methodology. RSM can be used to acquire the relationship between target variables, the output variables, and the predictor variables, the input variables, for relevant process optimizations. In addition, mathematical models of RSM may be built, with which the effects of the predictor variables can be analyzed. In addition, the relationship between the predictor and the target variables is shown in the following equation [31].

$$\eta = f(x_1, x_2, \dots, x_n) + \varepsilon \quad (1)$$

where η : in this research, the response is signified through a designated YP, f : the unknown function of response, x_1, x_2, \dots, x_n : the predictor variables in this analysis are denoted through nanosilica concentration in wt.%, the nanoclay concentration in wt.%, the bentonite concentration in wt.%, pressure in psi, and temperature in °F. n : the predictor variable's quantity. ε : statistical errors signifying added changeability sources not described via f .

The RSM utilizes a low-order polynomial equation to find a predetermined region of the predictor variables, which are later analyzed to locate the optimum values of predictor variables to find the best target [32]. Optimization using the RSM makes it quicker to gather experimental research results than conventional methods and a time-consuming one-factor-at-a-time approach [33]. Central Composite Design (CCD), D-optimal designs, Box–Behnken, and historical data design are the most used forms in the RSM [34]. The historical data design was used in this study because the data were collected from the experimental work [35].

The investigation in this study used the RSM technique for determining the nanosilica, nanoclay, and bentonite combined effect on YP. Drilling fluid is water based and contains calcium carbonate, subjected to various pressure and temperature environments. The aim was to define the relationship between inputs (nanosilica, nanoclay, bentonite concentrations, temperature, and pressure) and response YP. Using Design-Expert and Statistica software, new empirical correlations were created for YP predictions based on nanosilica, nanoclay, bentonite concentrations, pressure, and temperature. Apart from using statistical and Design-Expert

Table 1 Data range and statistical analysis of the collected data

Parameter	<i>T</i> (°F)	(<i>C_b</i>) (wt.%)	(<i>C_{ns}</i>) (wt.%)	(<i>C_{nc}</i>) (wt.%)	<i>P</i> (psi)	YP (lb/100 ft ²)
Minimum	85.00	0.00	0.00	0.00	14.70	0.00
Maximum	250.0	10.0	10.0	5.00	500.0	25.08
Mean	145.5	5.33	0.96	0.52	268.0	11.17
Median	150.0	6.66	0.00	0.00	300.0	11.42
Mode	85.00	0.00	0.00	0.00	300.0	9.67
Range	165.0	10.0	10.0	5.00	485.3	25.08
Skewness	0.610	− 0.21	2.62	2.61	− 0.25	− 0.14
Standard Deviation	51.36	4.54	2.26	1.32	129.8	4.49
Coefficient of variation	0.350	0.85	2.35	2.57	0.480	0.40

software, the method of regression was also employed to achieve the utmost data match [36]. The regression analysis contributes to determining the common relationship between the predictor and the target parameters, and a mathematical model is acquired, which fulfills the relationship of the objective functions with the test factor groups [37]. In addition, the regression method is also used to investigate the response surface behavior. The model for the response surface is generally conveyed through the ensuing equation:

$$Y = b_o + \sum_{i=1}^k b_i x_i + \sum_{i=1}^k b_{ii} x_i^2 + \sum_{i=1}^{k-1} \sum_{j=1}^k b_{ij} x_i x_j + e \quad (2)$$

where *Y*: the yield point; *X_i*, *X_j*: the affecting variables; *b_o*: the coefficient of model intercept. *b_j*, *b_{jj}*, and *b_{ij}*: linear, quadratic, and second-order terms' interaction coefficients, respectively. *K*: the independent parameter's quantity, and in this study, *k* = 5; *E*: error occurred [38].

Furthermore, analysis of variance (ANOVA) is applied to find to what degree the variable predictors like pressure, temperature, nanosilica, nanoclay, and bentonite concentrations influence the target variables and the YP in the regression study. Using ANOVA, statistical analyses were carried out to determine the roles of the predictor factors in response, i.e., the YP [39, 40].

3 Results and Discussion

3.1 Yield Point Correlation

The results obtained in this work show that the RSM model built for YP prediction was acceptable. For the final regression model, in the actual factor terms, the empirical

relationship between the YP and process variables is conveyed through the following quadratic equation:

$$y = 17.52127 - 0.047591X_1 + 0.513691X_2 + 1.05094X_3 + 4.93255X_4 - 0.017296X_2^2 - 0.038510X_3^2 - 0.800465X_4^2 - 0.003769X_1X_2 - 0.043229X_2X_4 \quad (3)$$

where *y* : yieldpoint; *X₁* : temperature(°F); *X₂* : BentoniteConcentration(wt.%); *X₃* : NanosilicaConcentration(wt.%); *X₄* : NanoclayConcentration(wt.%).

3.2 The Evaluation of the Yield Point Correlation

The YP model has been evaluated through ANOVA, diagnostics plots, Pareto charts, and fit statistics.

3.2.1 Analysis of Variance

An analysis was carried out at a 5% level of significance to detect the importance of the experimental factors. From ANOVA, i.e., the analysis of variance, the resultant *p*-values prove that every factor was important, having a 95% confidence level, and were acknowledged to be crucial parameters based on the test results, as Table 2 shows. Hence, Table 2 signifies the regression parameters of ANOVA for the YP's quadratic model of the predicted response surface.

The value of 320.38 as an *F*-value, in addition to the *p*-value of < 0.0001 or the low probability, indicates the significance of the model, as shown in Table 2. The < 0.05 value of *p* indicates the importance of model terms for confidence intervals of 95%. Nevertheless, > 0.1 value of *p* indicates the model term's insignificance [41, 42]. Due to the significance of all the terms, the model is enhanced to achieve greater accuracy and confidence levels.

Table 2 ANOVA for the yield point model

Source	Sum of squares	df	Mean square	F-value	p-value	
Model	1773.13	10	177.31	320.38	< 0.0001	Significant
A—Temperature	1068.71	1	1068.71	1931.00	< 0.0001	
B—Bentonite concentration	142.59	1	142.59	257.63	< 0.0001	
C—Nanosilica concentration	185.74	1	185.74	335.60	< 0.0001	
D—Nanoclay concentration	98.18	1	98.18	177.40	< 0.0001	
E—Pressure	3.33	1	3.33	6.02	0.0157	
AB	75.75	1	75.75	136.87	< 0.0001	
BD	10.15	1	10.15	18.34	< 0.0001	
B ²	2.57	1	2.57	4.64	0.0334	
C ²	5.65	1	5.65	10.2	0.0018	
D ²	140.56	1	140.56	253.97	< 0.0001	
Residual	63.09	114	0.5535			
Cor Total	1836.23	124				

Table 3 Validation properties of the YP correlation

R ²	Standard deviation	Mean	Coefficient of variation (%)	Adjusted R ²	Predicted R ²	Adequate precision
0.9656	0.744	11.32	6.57	0.963	0.957	81.732

3.2.2 F-Statistic Test

The f-statistic test was used to evaluate the RSM model to predict the YP. A F-statistic test can be applied to either support or reject a null hypothesis. The F-statistic test is discussed in section S1. F-statistic test in the Supporting Information.

3.2.3 Fit Statistics

The fit statistics analysis was used to evaluate the YP model, which includes R^2 , i.e., the determination coefficient and the predicted R^2 , as Table 3 shows. The values of 0.9656 for R^2 and 0.957 for predicted R^2 for the YP model show an improved connection between the measured results and the expected outcomes. The values of R^2 attained for the YP are more than 0.8, indicating that, through this empirical model, only 4.3% of the total dissimilarity is not fully explicable. Furthermore, Table 3 shows that the adequate precision value of 81.732 for the YP is greater than 4, which indicates sufficient model discrimination [42].

3.2.4 Pareto Chart

The utility of a Pareto chart is in finding the effects of interaction and the factor. The Pareto chart may acquire an

effect's importance and magnitude [43]. The Pareto chart was obtained using "Statistica" software. The Design-Expert and Statistica software yielded the same results in predicting the yield point (YP). However, their visualization capabilities are different; for example, the Pareto chart can be performed only in the Statistica software but not in the "Design-Expert". For this reason, we used the Statistica software in this study. The absolute value of a standardized effect is displayed through a Pareto chart. A vertical line in the chart denotes the confidence interval of 95%, and all factors of statistical significance cross this vertical line [44]. The standardized effects' Pareto charts for YP have shown all the factors as significant at the level of 0.05 concerning the model terms of YP, which is depicted in Fig. 2.

3.2.5 Diagnostics and Perturbation Plots

Diagnostic plots were used to evaluate the RSM model to predict the YP of the water-based drilling. Diagnostics plots include (1) normal plot, (2) predicted versus actual plot, and (3) residual versus predicted plot. A perturbation plot can be used to compare the effects of all factors at a point in the design space. The response can be plotted by changing only one factor over its range while holding the other factors constant. The diagnostic and perturbation plots are discussed

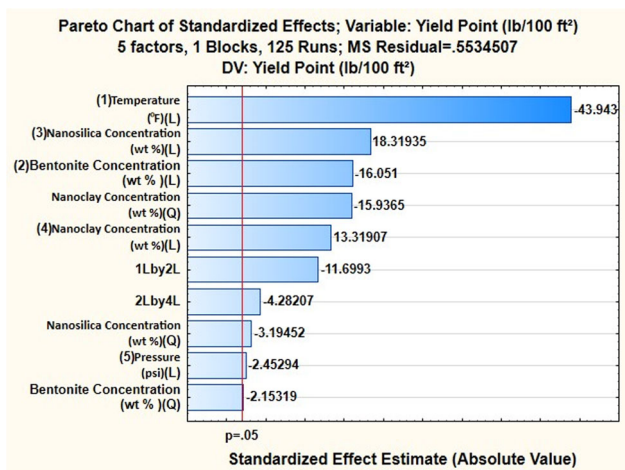


Fig. 2 Pareto chart

in section S2. Diagnostics plots and S.3 Perturbation plot in the Supporting Information.

3.3 Yield Point Model Verification

The YP model was validated against the measured data. Based on Fig. 3, it is evident that the YP model has high accuracy and more confidence. The proposed RSM model has an R^2 and RMSE of 0.9947 and 0.3429.

3.4 Effect of the Predictor Variables on YP

The YP model's contour and 3D plots of surface response were applied using Design-Expert and Statistica software to evaluate the interactive relationships of predictor variables,

Fig. 3 Predicted/ measured yield point (lb/100 ft²) for the verification

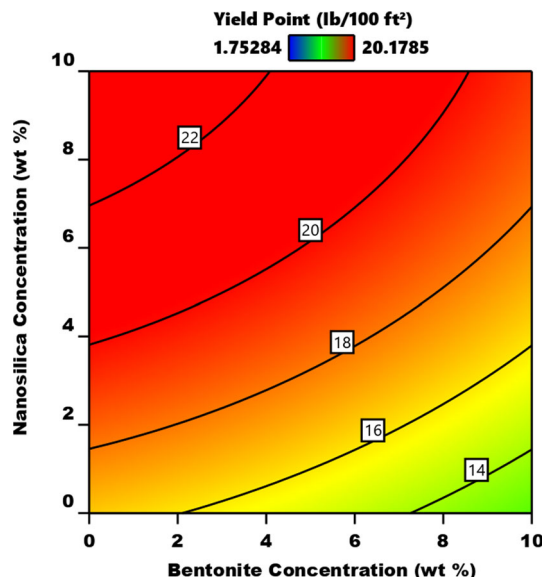
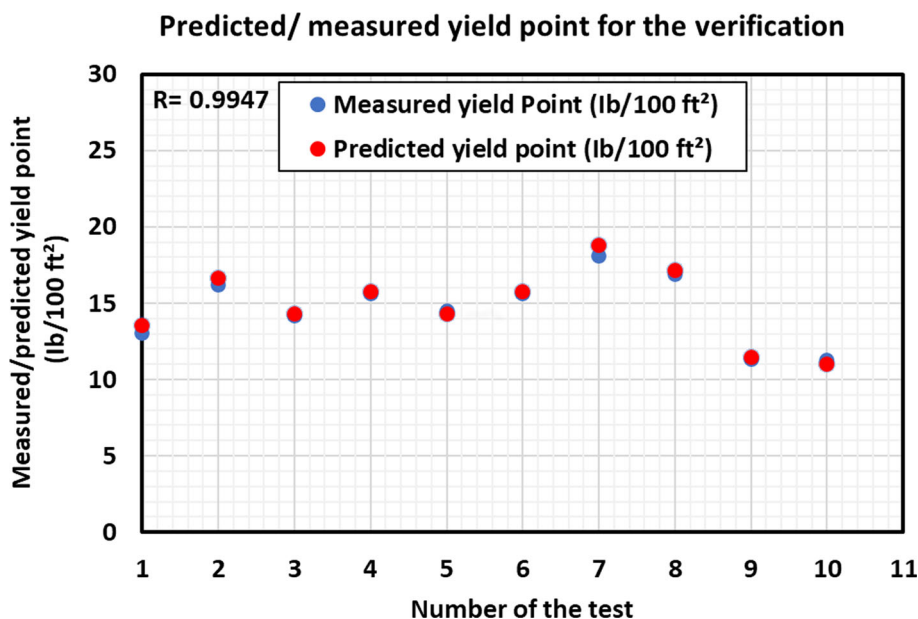


Fig. 4 Yield point's contour plot in relation to bentonite versus nanosilica concentrations

for instance, the concentrations of nanosilica, nanoclay, and bentonite (wt.%), the pressure (psi), temperature (°F), along with the response, i.e., the YP, as Figs. 4, 5, 6, 7, 8, 9, 10, 11, 12, 13 display.

3.4.1 Effect of Nanosilica and Bentonite Concentrations on the Yield Point

Figure 4 shows the YP's (i.e., lb/100 ft²) contour plot, a graphical diagram based on the nanosilica and bentonite. Figure S5 (Supporting information) shows the YP's (i.e.,

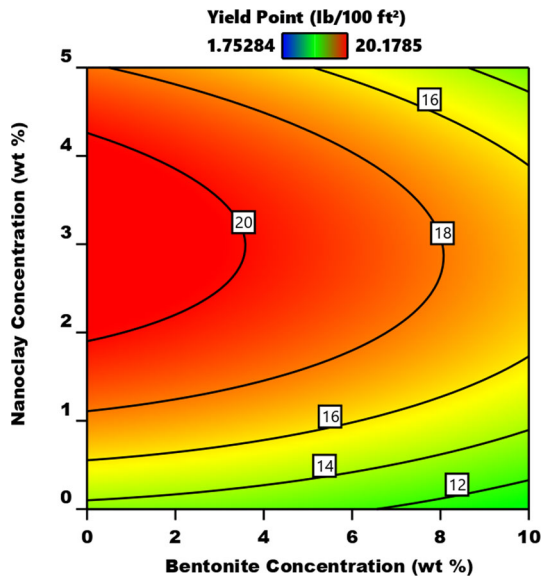


Fig. 5 Yield point's contour plot bentonite versus nanoclay concentrations

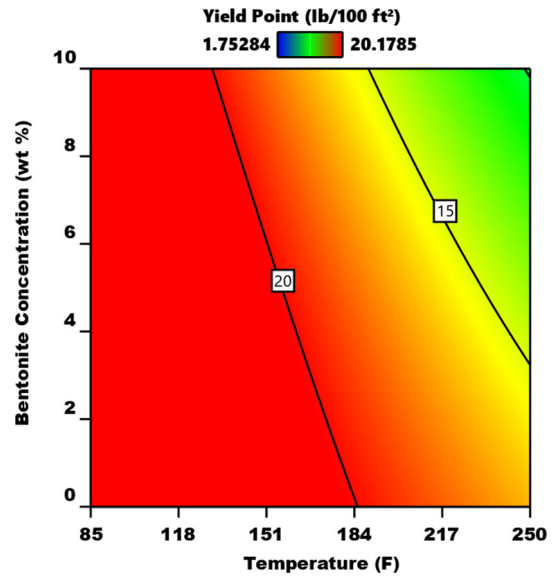


Fig. 7 Yield point's contour plot in relation to temperature versus concentration of bentonite

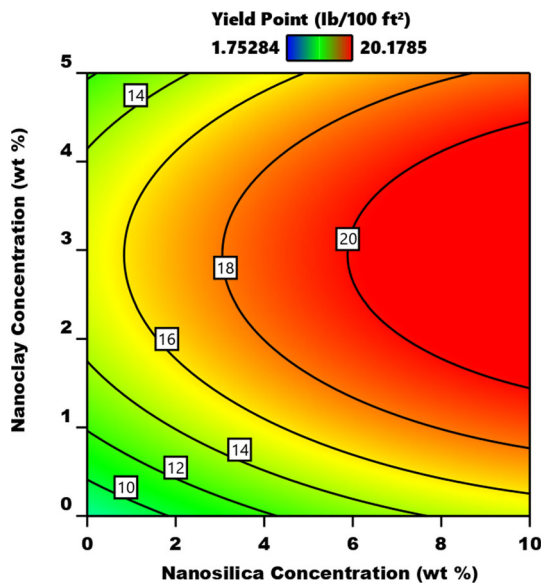


Fig. 6 Yield point's contour plot in relation to nanosilica versus of nanoclay concentrations

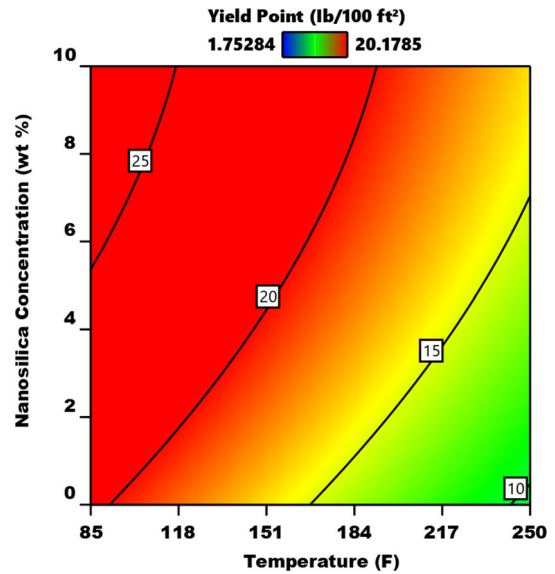


Fig. 8 Yield point's contour plot in relation to temperature versus concentration of nanosilica

Ib/100 ft²) 3D surface response plots are graphical diagrams based on the nanosilica and bentonite. Figures 4 and S5 show that the YP increases with the increase in nanosilica concentration. Due to having the same negative charge, the particles of bentonite and nanosilica repel one another within aqueous phases [45]. The YP decreases with increasing the bentonite concentration at the low nanosilica concentration in WBMs. YP showed increasing with increasing nanosilica only. As the nanosilica and bentonite are negatively charged, the YP does not increase when both nanosilica and bentonite increase simultaneously.

3.4.2 Effect of Nanoclay and Bentonite Concentrations on the Yield Point

Figure 5 shows the contour plot of YP versus bentonite concentration and nanoclay concentrations (wt.%), as the other parameters are maintained constant, i.e., nanoclay concentration, pressure, and temperature. Figure S6 shows the YP's (i.e., Ib/100 ft²) 3D surface response plots are graphical diagrams based on the nanoclay and bentonite. It is inferred in the figure that as the concentration of nanoclay (wt.%) increases from low to medium, YP increases due to the interaction of bentonite with nanoclay leading to an initial

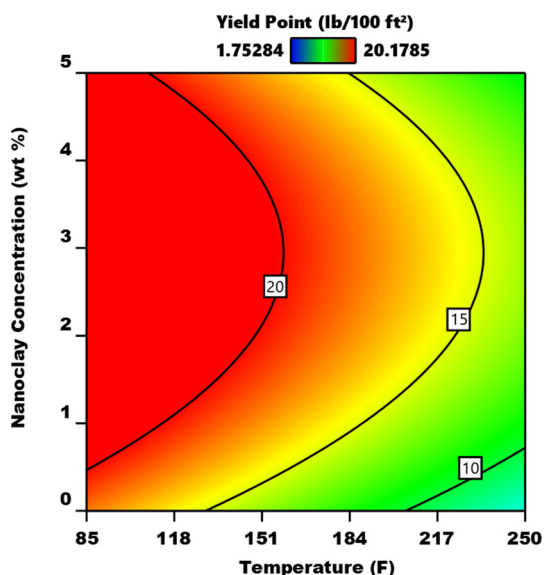


Fig. 9 Yield point's contour plot in relation to temperature versus concentration of nanoclay

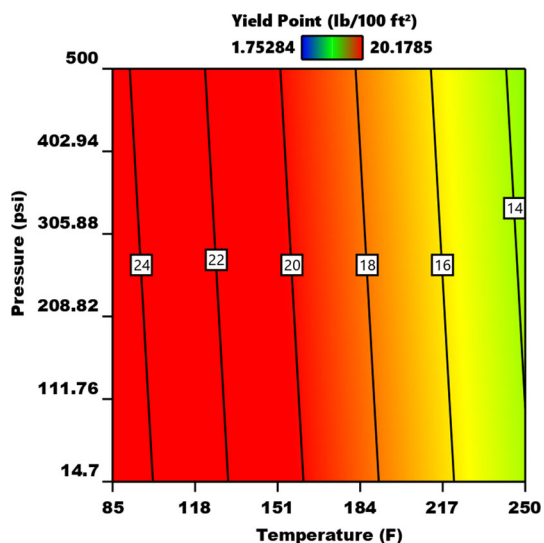


Fig. 10 Yield point's contour plot in relation to temperature versus pressure

YP increase. YP dropped as the nanoclay concentrations increased from medium to high concentrations. In 2015, Vipulanandan and Mohammed [46] employed 0–0.6 wt.% of nanoclay together with bentonite of 2, 8 wt.% at 25 °C–85 °C temperature or 77 °F–185 °F to attain the rheological improvement in the water-based mud. This study showed YP rise with an increase in the nanoclay and bentonite concentrations, but with temperature increase, their concentrations were lowered and decreased. When the nanoclay concentration is high, agglomeration of the nanoparticles, i.e., the nanoclay, can occur, reducing its capacity for enhancing suspension [47].

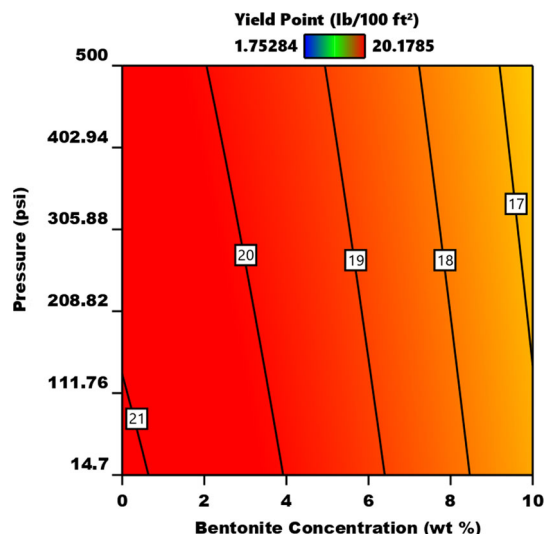


Fig. 11 Yield point's contour plot in relation to the concentration of bentonite versus pressure

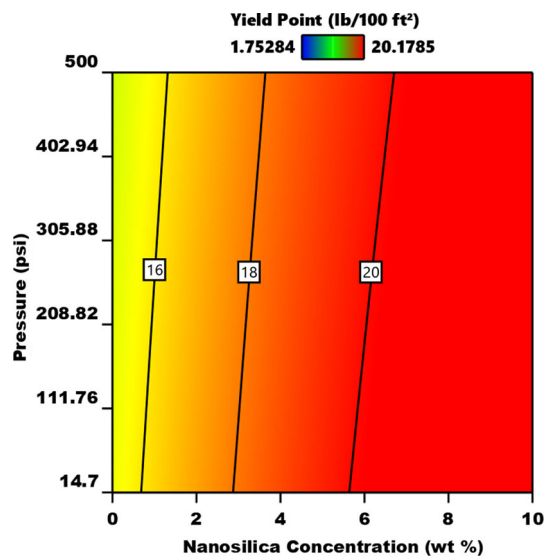


Fig. 12 Yield point's contour plot in relation to concentration of nanosilica versus pressure

3.4.3 Effect of Nanosilica and Nanoclay Concentrations on the Yield Point

In Fig. 6 (the contour plot), YP is dependent on the wt.% percentage concentrations of nanoclay and nanosilica while the other parameters are held constant, viz. the concentration of bentonite in wt.%, the pressure value in psi, and the temperature value in °F. Figure S7 shows the YP's (i.e., Ib/100 ft²) 3D surface response plots are graphical diagrams based on the nanosilica and nanoclay. So, Figs. 6 and S7 specify when the nanoclay concentration ranges from low wt.% to medium wt.%, an initial increase in the YP occurs due to the rise in the percentages of the concentrations of nanosilica and nanoclay. Nonetheless, concentrations of nanoclay

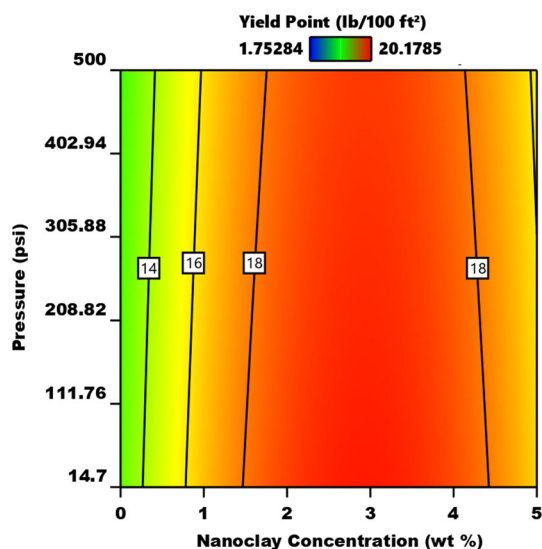


Fig. 13 Yield point's contour plot in relation to the concentration of nanoclay versus pressure

range from the medium wt.% to high wt.%, with increasing concentrations of nanosilica and nanoclay; YP shows declining. These results match equitably with the results of Agarwal et al. [48], who 2011 examined the impacts of nanosilica on the rheology of drilling fluids. They showed that a concentration increase of the combined nanosilica and nanoclay in lower concentrations can increase the drilling fluid viscosity. Moreover, low nanoclay concentrations enable the nanosilica and nanoclay nanoparticles to improve the suspension. When the nanoclay concentrations are high, agglomeration of nanosilica and nanoclay nanoparticles may occur, reducing their enhanced suspension ability [47]. Consequently, the water-based drilling fluid's YP decreased to a nanoclay concentration of medium to a high wt %.

3.4.4 Effect of Temperature (°F) and Concentration of Bentonite on the Yield Point

In Fig. 7, it is seen that the YP's contour plot is reliant on wt.% bentonite concentration and temperature (°F), while the rest of the parameters remained constant. Figure S8 shows the YP's (i.e., lb/100 ft²) 3D surface response plots, which are graphical diagrams based on temperature and bentonite. An increase in the bentonite concentration with a decrease in temperature increases YP. By expanding the bentonite concentrations, the YP of the drilling fluid (water based) was enlarged [49]. Bentonite attaches to the water surfaces, which are charged positively, owing to the face surface of bentonite, which is charged negatively, through the electrostatic attraction; hence, the rheological properties, namely YP of the drilling fluid (water based), are enhanced [50].

3.4.5 Effect of Concentration of Nanosilica and Temperature on the Yield Point

Figure 8 illustrates the contour plot of the variation in the YP versus temperature and nanosilica concentration in wt.%. Figure S9 displays the YP's (i.e., lb/100 ft²) 3D surface response plots are graphical diagrams based on the temperature and nanosilica. Figures 8 and S9 show that the YP increases with a decrease in temperature and an increase in nanosilica concentration. Ismail et al. [51] also noticed the positive effect of the nanosilica on the WBDF's rheology. Increasing the concentration of nanosilica increases YP. The nanosilica concentration enhances the rheological properties, such as YP, due to the rising surface forces and the contact surface because of the robust hydrogen bonding created with the other components of the drilling fluid [52].

3.4.6 Effect of Concentration of Nanoclay and Temperature on the Yield Point

Figure 9 shows the contour plot of the cumulative impact of wt.% concentration of nanoclay and the effect of temperature (°F) on YP. Figure S10 shows the YP's (i.e., lb/100 ft²) 3D surface response plots, which are graphical diagrams based on temperature and nanoclay. It is seen in Fig. 9 and S10 that at different temperatures, the concentration increases of nanoclay in wt.% lead to a greater initial YP; however, a decrease is shown after that concentration. Also, when the temperatures are low, a low to medium increase in concentrations of nanoclay in wt.% causes an increase in the YP. However, with the continuing rise in the percentage of nanoclay from medium to high, a reduction in the YP can be recognized.

3.4.7 Effect of Pressure and Temperature on the Yield Point

Figure 10 shows the contour plot of the effect of temperature (°F) and pressure (psi) on YP. The YP is unaffected, while other variables are kept constant with the pressure and temperature increase, and other variables are steady. Figure S11 shows the YP's (i.e., lb/100 ft²) 3D surface response plots, which are graphical diagrams based on temperature and pressure. As temperature increases, the cohesive forces between the molecules decrease; thus, the forces of attraction between the particles decrease, reducing the liquid viscosity. In conclusion, the YP decreases with the increase in temperature. However, in this study, the pressure was not high enough to increase the cohesive forces between the molecules of the particles of the drilling fluids. Hence, the YP is shown as pressure independent. Wang et al. [53] mentioned that temperature significantly influenced YP in WBMs. They reported that the yield point decreased with increasing temperature.

3.4.8 Effect of Pressure and Concentration of Bentonite on the Yield Point

Figure 11 shows the contour plot that at different concentrations of bentonite (wt.%), with changing pressure (psi) and other properties, viz. the temperature ($^{\circ}\text{F}$), the nanoclay concentration (wt.), and the nanosilica concentration (wt.%), as constants. Figure S12 shows the YP's (i.e., lb/100 ft²) 3D surface response plots, which are graphical diagrams based on pressure and bentonite. Figures 11 and S12 show that the flat response surface indicates that pressure has no significant effect on the WBM's YP. As discussed before, the pressure was not high enough to significantly increase the cohesive forces between the molecules of the bentonite, nanosilica, and nanoclay particles.

3.4.9 Effect of Pressure and Concentration of Nanosilica on the Yield Point

Figure 12 shows the contour plot of the effects of the concentration of nanosilica in wt.% and the pressure on YP, as the remaining factors are maintained at fixed values. Figure S13 shows the YP's (i.e., lb/100 ft²) 3D surface response plots, which are graphical diagrams based on the pressure and nanosilica. As shown in Figs. 12 and S13, the YP increases with the increase in the nanosilica concentration but remains constant with the increase in pressure. This observation is contrary to what was reported by Li et al. [54], who stated that the YP could be enhanced by adding nanosilica to the drilling fluid. It is noted that this pressure independence is due to the low values of pressure used.

3.4.10 Effect of Pressure and Concentration of Nanoclay on the Yield Point

Figure 13 shows the contour plot of the variation in the YP with changing the wt.% concentration of nanoclay and the pressure. Figure S14 shows the YP's (i.e., lb/100 ft²) 3D surface response plots are graphical diagrams based on the pressure and nanoclay. Figures 13 and S14 indicate that with increasing the nanoclay concentration and pressure, the YP increases at low to medium nanoclay concentrations. However, from medium to high concentration, a reverse trend is shown. Again, the pressure independency of the YP at constant nanoclay concentration can be observed.

3.5 The Superiority of the Proposed Model Over Existing Models

A total of 23 models have been published, as shown in Table 4. The majority (13 out of 23) of the published work was based on the ANN method. The RSM was implemented

in this study, which stands out as previous models mostly utilized ANN. Although some models used ANFIS, DT, and RF methods, none employed RSM. This novel modeling method can complement the current predictive tools effectively. RSM is considered significantly more accurate than previous techniques. In addition, the RSM models are often polynomial equations that are easier to interpret and apply for prediction.

The proposed RSM is the best model to predict the YP, with the highest R^2 of 0.9947. In addition, the proposed RSM model was built based on 1256 data points. Ashadevi et al. [16] model has an R^2 value of 0.99 to predict the YP of the oil-based drilling fluid; however, the model was built based on 40 data points, as shown in Table 4. Mengich et al. [14] model has an R^2 value of 0.7013, the lowest value in Table 4. Tchameni et al. [22] and Davoodi et al. [24] models have R^2 values of 0.807 and 0.8672, respectively. Table 4 shows that other models have R^2 values higher than 0.9.

Ashadevi et al. [16] and Razi et al. [2] models have RMSE values of 0.01 and 0.0948; however, their models were created based on 40 and 80 data points. Davoodi et al. [24], Gouda et al. [13], Al-Obaidi et al. [15], Tchameni et al. [22], Mengich et al. [14] models have RMSE values of 0.6357, 0.76, 0.891, 2.9878, 10.149, respectively. Abdelaal et al. [18] RF and DT models have RMSE values of 5.66 and 3.02 for R_{600} and R_{300} and 5.85 and 3.0 for R_{600} and R_{300} , respectively. In contrast, the proposed RSM model has an RMSE of 0.3429; the proposed RSM model was developed based on more data points to cover wider data ranges compared to other models.

Existing studies used input parameters such as the concentration of starch in the mud and potash, temperature, the Marsh funnel viscosity, solid content, mud density, the water volume, and the concentrations of bentonite and biopolymer in different ranges to predict the YP (Table 4). In comparison, the proposed model was developed based on pressure (P), temperature (T), concentrations of nanosilica (C_{ns}), concentrations of nanoclay (C_{nc}), and concentrations of bentonite (C_b) in the ranges (14.70–500) psi, (85–250) $^{\circ}\text{F}$ (0–10) wt.%, (0–5) wt.%, (0–10) wt.%. Thus, the input parameters used in the proposed model are more relevant and greater in numbers.

Therefore, the proposed model was developed based on P , T , C_{ns} , C_{nc} , and C_b as inputs, which were more relevant because they affect the YP. A total of 1256 data points were used to create the proposed RSM model to cover more comprehensive data ranges. Moreover, this study used RSM, a unique technique, to predict the drilling fluid's YP. Furthermore, the proposed RSM model has the highest accuracy (R^2 of 0.9947) in predicting the drilling fluid's YP.

Table 4 Comparison between the recent and proposed methods

Model/reference	Technique	Water/oil-based drilling fluid	Inputs	Number of data	Root mean square error (RMSE)	R^2	Others
Razi et al. [4]	An artificial neural network (ANN)	Water based	Shear rate, temperature, and starch concentration	80 data points	0.0948	0.986	–
Elkatatny et al. [5]	ANN	Oil based	The Marsh funnel viscosity, the density of the drilling fluid, and the solid content	9000 data points	–	–	A mathematical model that is obtained from the weights and biases
Elkatatny and Mahmoud [6]	ANN	Water based	The Marsh funnel viscosity, solid content, and mud density	3000 data points	–	0.98	A mathematical model that is obtained from the weights and biases
Abdelgawad et al. [7]	ANN	Bentonite spud mud	The Marsh funnel viscosity, solid content, and mud density in the ranges (26–120) s, (0–24)%, (63–80) lb/ft ³	2000 data points	–	0.94	A mathematical model that is obtained from the weights and biases
Gowida et al. [8]	ANN	CaCl ₂ brine	The Marsh funnel viscosity and mud density in the ranges (26–135) s/quart and (64–155) lb/ft ³	515 field data	–	0.97	A mathematical model that is obtained from the weights and biases
Gomaa et al. [9]	ANN	High-overbalanced bridging mud	The Marsh funnel viscosity and mud density in the ranges (42–120) s/quart and (43–119) lb/ft ³	1200 data points	–	0.97 and 0.96 for R300 and R600	A mathematical model that is obtained from the weights and biases
Oguntade et al. [10]	ANN	Mud with modified biopolymer	The water volume, the concentrations of bentonite and biopolymer	100 data set	–	0.92 and 0.99 for 15 and 8 neurons	–
Gowida et al. [11]	ANN	High-bentonite mud	The Marsh funnel viscosity and mud density in the ranges (45–150) s/quart and (64–73) lb/ft ³	200 data points	–	0.92	A mathematical model that is obtained from the weights and biases
Alsabaa and Elkatatny [12]	ANN	Oil based	The density of the drilling fluid and Marsh funnel in the ranges (76–120) pcf and (44–20) s	383 samples	–	0.91	A mathematical model that is obtained from the weight and biases



Table 4 (continued)

Model/reference	Technique	Water/oil-based drilling fluid	Inputs	Number of data	Root mean square error (RMSE)	R ²	Others
Gouda et al. [13]	ANN	Invert emulsion drilling fluid	Mud temperature, Marsh funnel viscosity, solid content percentage, and mud density in the ranges (60–170)°F, (40–85) sec/qrt, (14.5–36.6)%, (10.2–13.85), respectively	407 datasets	0.76	0.94	A mathematical model that is obtained from the weight and biases
Mengich et al. [14]	ANN	Water based	Mud density, percent solids content, and Marsh funnel	557 data values	10.149	0.7013	–
Al-Obaidi et al. [15]	ANN	water based	The mud weight (MW), Marsh Funnel (MF), and solid content (S%)	–	0.891	0.90	–
Ashadevi et al. [16]	ANN3	Oil based	The temperature, mud density, and shear rate	40 data points	0.01	0.99	–
Alsabaa et al. [17]	Adaptive neuro-fuzzy inference system (ANFIS)	Invert emulsion mud	The Marsh funnel viscosity and mud density in the ranges (45–98) s/ quart and (67–98) lb/ft ³	741 data points	–	0.91	–
Abdelaal et al. [18]	ANFIS	Oil based	The mud density (MD) and Marsh funnel viscosity (MFV) in the ranges (70–120) pcf and (27–120) sec/ quart	550 data points	–	0.96	–
Oliveira [20]	Nonlinear regression	oil based	Pressure and temperature in the ranges (200–450) °F and (5000–40000) psig	–	–	0.9271	–
Fakoya and Ahmed [21]	Nonlinear regression analysis	Oil based	The volume fraction of dispersed phase and temperature in the range (24–87) °C	–	–	–	–

Table 4 (continued)

Model/reference	Technique	Water/oil-based drilling fluid	Inputs	Number of data	Root mean square error (RMSE)	R^2	Others
Tchameni et al. [22]	Multiple nonlinear regression and ANN methods	Oil biodiesel-modified WBM based	Biodiesel content and aging temperature in the range (28–180) °C	20 data points	2.9878	0.807	–
Ye et al. [23]	The regression	Oil based	Temperature and pressure in the ranges (60–160) °C and (0.1–150) MPa	56 datasets	–	–	–
Davoodi et al. [24]	The cuckoo optimization algorithm	Water based	The fluid density, solid percentage, and Marsh funnel viscosity in the ranges (70–148) pcf, (2.7–47.0)%, (36.0–78.0) sec/quart	1160 datasets	0.6357	0.8672	–
Abdelaal et al. [19]	Random forest (RF), decision tree (DT)	Oil based	The mud density (MD) and Marsh funnel viscosity (MFV)	533 data points	RF: 5.66 and 3.02 for R600 and R300 DT: 5.85 and 3.0 for R600 and R300	0.954 and 0.955	–
Okumo and Isehunwa [25]	Factorial design	Water based	Concentration of starch in the mud and potash and temperature	–	–	–	Coefficient of Variance (COV) = 6.435%
Igwilo et al. [26]	The least square and Gaussian elimination method	Oil-based	Mud temperature in the ranges (80–180)°F	–	–	0.8955, 0.9911, 0.9475, 0.9905, and 0.9846	–
The proposed model	RSM	Water based	Pressure (P), temperature (T), concentrations of nanosilica (C_{ns}), concentrations of nanoclay (C_{nc}), and bentonite (C_b) in the ranges (14.70–500) psi, (85–250) °F, (0–10) wt.%, (0–5) wt.%, (0–10) wt.%	1256 data points	0.3429	0.9947	–



4 Summary and Conclusions

To sum it up, in this work, a YP correlation was established based on bentonite, nanosilica, nanoclay concentrations, temperature, and pressure, for which the response surface methodology, i.e., RSM, was applied. This developed correlation was analyzed statistically and validated through different methods, such as fit statistics, ANOVA, diagnostics plots, and Pareto charts, to enhance its accuracy and a high degree of confidence for oil and gas industrial applications. Following the validation, the YP prediction is derived from the developed correlation with the Pearson correlation coefficient (R) of 0.9947, demonstrating a fitting match between the measured data and predicted data. The predicted and measured data showed proper matching, which established the suitability of the developed correlation for yield points.

The influence of the predictor variables: the bentonite concentration, nanoclay concentration, nanosilica concentration, temperature, and pressure on the YP, was investigated. Statistical significance was evident from the 3D response surface plots and the interactions of the system's variables. Furthermore, the findings from the 3D response surface plots highlight the ensuing extrapolations:

- 1- YP decreases with increasing temperature.
- 2- At low pressures of less than 500 psi, the pressure had a negligible effect on the YP of the water-based drilling fluids.
- 3- For the concentrations of nanoclay ranging from low wt.% to medium wt.%, with an increase in the concentration of nanoclay, YP initially increased due to the heightened bentonite interactions with the nanoclay. After that, as the nanoclay concentration alters from medium wt.% range to high wt.% ranges, the YP showed declining.
- 4- Initially, the YP showed increasing due to the nanosilica interacting with the nanoclay. When the nanoclay concentrations were at medium wt.% toward high wt.%, the higher concentrations of both nanoclay and nanosilica caused the YP to decline.

Supplementary Information The online version contains supplementary material available at <https://doi.org/10.1007/s13369-024-09415-6>.

Acknowledgements The authors sincerely thank the Yayasan Universiti Teknologi PETRONAS (Cost Centre: 015LC0-451) at Universiti Teknologi PETRONAS for supporting this study.

Funding Universiti Teknologi Petronas, Cost Centre: 015LC0-451, Syed Mohammad Mahmood.

References

1. Bourgoyne, A.T.; Millheim, K.K.; Chenevert, M.E.; Young, F.S.: Applied drilling engineering (Vol. 2): society of petroleum engineers Richardson (1991)
2. Song, K.; Wu, Q.; Li, M.; Ren, S.; Dong, L.; Zhang, X.; Lei, T.; Kojima, Y.: Water-based bentonite drilling fluids modified by novel biopolymer for minimizing fluid loss and formation damage. *Colloids Surf. A Physicochem. Eng. Asp.* **507**, 58–66 (2016)
3. Perween, S.; Thakur, N.K.; Beg, M.; Sharma, S.; Ranjan, A.: Enhancing the properties of water based drilling fluid using bismuth ferrite nanoparticles. *Colloids Surf. A Physicochem. Eng. Asp.* **561**, 165–177 (2019)
4. Razi, M.M.; Mazidi, M.; Razi, F.M.; Aligolzadeh, H.; Niazi, S.: Artificial neural network modeling of plastic viscosity, yield point, and apparent viscosity for water-based drilling fluids. *J. Dispers. Sci. Technol.* **34**, 822–827 (2013). <https://doi.org/10.1080/01932691.2012.704746>
5. Elkhatny, S.; Tariq, Z.; Mahmoud, M.: Real time prediction of drilling fluid rheological properties using Artificial Neural Networks visible mathematical model (white box). *J. Pet. Sci. Eng.* **146**, 1202–1210 (2016)
6. Elkhatny, S.; Mahmoud, M.: Real time prediction of the rheological parameters of NaCl water-based drilling fluid using artificial neural networks. *Soc. Pet. Eng. SPE Kingd. Saudi Arab. Annu. Tech. Symp. Exhib.* **2017**, 1726–1740 (2017). <https://doi.org/10.2118/187976-ms>
7. Abdelgawad, K.; Elkhatny, S.; Moussa, T.; Mahmoud, M.; Patil, S.: Real-time determination of rheological properties of spud drilling fluids using a hybrid artificial intelligence technique. *J. Energy Resour. Technol.* **141**, 32908 (2019)
8. Gowida, A.; Elkhatny, S.; Ramadan, E.; Abdurraheem, A.: Data-driven framework to predict the rheological properties of CaCl₂ brine-based drill-in fluid using artificial neural network. *Energies (Basel)* **12**, 1880 (2019)
9. Gomaa, I.; Elkhatny, S.; Abdurraheem, A.: Real-time determination of rheological properties of high over-balanced drilling fluid used for drilling ultra-deep gas wells using artificial neural network. *J. Nat. Gas Sci. Eng.* **77**, 103224 (2020)
10. Oguntade, T.; Ojo, T.; Efajemue, E.; Oni, B.; Idaka, J.: Application of ANN in predicting water based mud rheology and filtration properties. In: *SPE Nigeria Annual International Conference and Exhibition. SPE*, p. D013S009R012 (2020)
11. Gowida, A.; Elkhatny, S.; Abdelgawad, K.; Gajbhiye, R.: Newly developed correlations to predict the rheological parameters of high-bentonite drilling fluid using neural networks. *Sensors* **20**, 2787 (2020)
12. Alsabaa, A.; Elkhatny, S.: Improved tracking of the rheological properties of max-bridge oil-based mud using artificial neural networks. *ACS Omega* **6**, 15816–15826 (2021)
13. Gouda, A.; Khaled, S.; Gomaa, S.; Attia, A.M.: Prediction of the rheological properties of invert emulsion mud using an artificial neural network. *ACS Omega* **6**, 32948–32959 (2021)
14. Mengich, H.; Kabugu, M.; Ondiaka, M.N.: Prediction of rheological properties of recirculating water-based drilling mud in geothermal exploration using artificial neural networks with tensor flow. *Eur. J. Energy Res.* **2**, 49–56 (2022)
15. Al-Obaidi, A.K.; Majidi, H.S.; Jweeg, M.J., Hadi, F.A., Jasim, D.J., Ellafi, A.: Artificial intelligent for real-time prediction of rheological drilling mud Properties. *Iraqi Geol. J.* 147–161 (2024)
16. Ashadevi, U.; Sutha, S.; Ramaswamy, A.: AI-powered predictive model for enhanced drilling control performance using invert emulsion fish oil-based drilling mud. *IFAC-PapersOnLine* **57**, 403–408 (2024)
17. Alsabaa, A.; Gamal, H.; Elkhatny, S.; Abdurraheem, A.: Real-time prediction of rheological properties of invert emulsion mud using adaptive neuro-fuzzy inference system. *Sensors* **20**, 1669 (2020)
18. Abdelaal, A.; Elkhatny, S.; Ibrahim, A.: Viscometer readings prediction of flat rheology drilling fluids using adaptive neuro-fuzzy inference system. In: *SPE Middle East Oil and Gas Show and Conference. SPE*, p. D021S073R004 (2023)



19. Abdelaal, A.; Ibrahim, A.F.; Elkhatny, S.: Data-driven framework for real-time rheological properties prediction of flat rheology synthetic oil-based drilling fluids. *ACS Omega* **8**, 14371–14386 (2023)
20. Oliveira, R.: Long-range description of rheological properties of a high-pressure hightemperature oil-based drilling fluid. Master of Science Thesis, Texas A&M University (2016)
21. Fakoya, M.F.; Ahmed, R.M.: A generalized model for apparent viscosity of oil-based muds. *J. Pet. Sci. Eng.* **165**, 777–785 (2018)
22. Tchameni, A.P.; Zhao, L.; Ribeiro, J.X.F.; Li, T.: Predicting the rheological properties of waste vegetable oil biodiesel-modified water-based mud using artificial neural network. *Geosyst. Eng.* **22**, 101–111 (2019)
23. Ye, Y.; Fan, H.; Liu, Y.: A new approach for predicting the rheological properties of oil-based drilling fluids under high temperature and high pressure based on a parameter-free method. *Appl. Sci.* **13**, 8592 (2023)
24. Davoodi, S.; Mehrad, M.; Wood, D.A.; Ghorbani, H.; Rukavishnikov, V.S.: Hybridized machine-learning for prompt prediction of rheology and filtration properties of water-based drilling fluids. *Eng. Appl. Artif. Intell.* **123**, 106459 (2023)
25. Okumo, I., Isehunwa, S.O.: Prediction of the viscosity of a water-base mud treated with cassava starch and potash at varying temperatures using factorial design. In: Nigeria Annual International Conference and Exhibition. OnePetro (2007)
26. Igwilo, K.; Godspower, I.; Nnanna, O.; Osueke, G.; Jude, O.; Anawe, P.: Modeling the effects of temperature on oil base mud viscosity using polynomial equation. *Int. J. Pet. Petrochem. Eng.* **3**, 16–22 (2017)
27. Breig, S.J.M.; Luti, K.J.K.: Response surface methodology: a review on its applications and challenges in microbial cultures. *Mater Today Proc.* **42**, 2277–2284 (2021)
28. Moraveji, M.K.; Naderi, M.: Drilling rate of penetration prediction and optimization using response surface methodology and bat algorithm. *J. Nat. Gas Sci. Eng.* **31**, 829–841 (2016)
29. Alakbari, F.S.; Mohyaldinn, M.E.; Ayoub, M.A.; Muhsan, A.S.; Hassan, A.: Apparent and plastic viscosities prediction of water-based drilling fluid using response surface methodology. *Colloids Surf. A Physicochem. Eng. Asp.* **616**, 126278 (2021)
30. Alakbari, F., Elkhatny, S., Kamal, M.S., Mahmoud, M.: Optimizing the gel strength of water-based drilling fluid using clays for drilling horizontal and multi-lateral wells. In: SPE Kingdom of Saudi Arabia Annual Technical Symposium and Exhibition held in Dammam, Saudi Arabia, 23–26 April 2018, SPE-192191-MS (2018)
31. Myers, R.H.; Montgomery, D.C.; Anderson-Cook, C.M.: *Response Surface Methodology: Process and Product Optimization Using Designed Experiments*. John Wiley & Sons, Hoboken (2016)
32. Ceylan, H.; Kubilay, S.; Aktas, N.; Sahiner, N.: An approach for prediction of optimum reaction conditions for laccase-catalyzed bio-transformation of 1-naphthol by response surface methodology (RSM). *Bioresour. Technol.* **99**, 2025–2031 (2008)
33. Alim, M.A.; Lee, J.-H.; Akoh, C.C.; Choi, M.-S.; Jeon, M.-S.; Shin, J.-A.; Lee, K.-T.: Enzymatic transesterification of fractionated rice bran oil with conjugated linoleic acid: optimization by response surface methodology. *LWT-Food Sci. Technol.* **41**, 764–770 (2008)
34. Asghar, A.; Abdul Raman, A.A.; Daud, W.M.A.W.: A comparison of central composite design and Taguchi method for optimizing Fenton process. *Sci. World J.* **2014**(1), 869120 (2014)
35. Alakbari, F.S., Mohyaldinn, M.E., Ayoub, M.A., Muhsan, A.S., Abdulkadir, S.J., Hussein, I.A., Salih, A.A.: Prediction of critical total drawdown in sand production from gas wells: machine learning approach. *Can. J. Chem. Eng.* (2022)
36. Dawud, E.R.; Shakya, A.K.: HPLC-PDA analysis of ACE-inhibitors, hydrochlorothiazide and indapamide utilizing design of experiments. *Arab. J. Chem.* **12**, 718–728 (2019)
37. Deng, L.; Cai, C.S.: Bridge model updating using response surface method and genetic algorithm. *J. Bridge Eng.* **15**, 553–564 (2010)
38. Shojai, A.; Fattahi, M.; Jorfi, S.; Ghasemi, B.: Hydrothermal synthesis of Fe-TiO₂-Ag nano-sphere for photocatalytic degradation of 4-chlorophenol (4-CP): investigating the effect of hydrothermal temperature and time as well as calcination temperature. *J. Environ. Chem. Eng.* **5**, 4564–4572 (2017)
39. Adalarasan, R.; Santhanakumar, M.; Rajmohan, M.: Application of Grey Taguchi-based response surface methodology (GT-RSM) for optimizing the plasma arc cutting parameters of 304L stainless steel. *Int. J. Adv. Manuf. Technol.* **78**, 1161–1170 (2015)
40. Derdour, F.Z.; Kezzar, M.; Khochemane, L.: Optimization of penetration rate in rotary percussive drilling using two techniques: Taguchi analysis and response surface methodology (RMS). *Powder Technol.* **339**, 846–853 (2018)
41. Zabeti, M.; Daud, W.M.A.W.; Aroua, M.K.: Biodiesel production using alumina-supported calcium oxide: an optimization study. *Fuel Process. Technol.* **91**, 243–248 (2010)
42. Design-Expert, 2019: *Design-Expert® 2019 User's Guide for Design-Expert Software*. Stat-Ease Incorporation, Minneapolis, MN (2019)
43. Antony, J.: *Design of Experiments for Engineers and Scientists*. Elsevier, Amsterdam (2023)
44. Umanath, K.; Palanikumar, K.; Selvamani, S.T.: Analysis of dry sliding wear behaviour of Al6061/SiC/Al₂O₃ hybrid metal matrix composites. *Compos. B Eng.* **53**, 159–168 (2013)
45. Elochukwu, H.; Gholami, R.; Dol, S.S.: An approach to improve the cuttings carrying capacity of nanosilica based muds. *J. Pet. Sci. Eng.* **152**, 309–316 (2017)
46. Vipulanandan, C.; Mohammed, A.: Effect of nanoclay on the electrical resistivity and rheological properties of smart and sensing bentonite drilling muds. *J. Pet. Sci. Eng.* **130**, 86–95 (2015)
47. Elkhatny, S.; Kamal, M.S.; Alakbari, F.; Mahmoud, M.: Optimizing the rheological properties of water-based drilling fluid using clays and nanoparticles for drilling horizontal and multi-lateral wells. *Appl. Rheol.* **28**(4), 201843606 (2018)
48. Agarwal, S., Tran, P., Soong, Y., Martello, D.K., Gupta, R.: Research shows benefits of adding nanoclay, nanosilica to oil-based hp/ht drilling fluids. *Am. Oil Gas Report*. (2011)
49. Mahto, V.; Sharma, V.P.: Rheological study of a water based oil well drilling fluid. *J. Pet. Sci. Eng.* **45**, 123–128 (2004)
50. Li, M.-C.; Wu, Q.; Song, K.; French, A.D.; Mei, C.; Lei, T.: pH-responsive water-based drilling fluids containing bentonite and chitin nanocrystals. *ACS Sustain. Chem. Eng.* **6**, 3783–3795 (2018)
51. Ismail, A.R.; Aftab, A.; Ibupoto, Z.H.; Zolkifile, N.: The novel approach for the enhancement of rheological properties of water-based drilling fluids by using multi-walled carbon nanotube, nanosilica and glass beads. *J. Pet. Sci. Eng.* **139**, 264–275 (2016)
52. Shu, H.; Li, X.; Zhang, Z.: Surface modified nano-silica and its action on polymer. *Prog. Chem.* **20**, 1509 (2008)
53. Wang, F.; Tan, X.; Wang, R.; Sun, M.; Wang, L.; Liu, J.: High temperature and high pressure rheological properties of high-density water-based drilling fluids for deep wells. *Pet. Sci.* **9**, 354–362 (2012)
54. Li, S., Osisanya, S., Haroun, M.: Development of new smart drilling fluids using nano-materials for unconventional reservoirs (2016)

Springer Nature or its licensor (e.g. a society or other partner) holds exclusive rights to this article under a publishing agreement with the author(s) or other rightsholder(s); author self-archiving of the accepted manuscript version of this article is solely governed by the terms of such publishing agreement and applicable law.